RFID landslide monitoring : long-term outdoor signal processing and phase unwrapping

Arthur Charléty, Mathieu Le Breton, Laurent Baillet, Eric Larose

RFID landslide monitoring : long-term outdoor signal processing and phase unwrapping

Arthur Charléty[1], Mathieu Le Breton[2], Laurent Baillet[1], and Eric Larose[1]

[1] Université Grenoble Alpes, Université Savoie Mont Blanc, CNRS, IRD, Université Gustave Eiffel, ISTerre, Grenoble, France
[2] Géolithe, Crolles, France

***Abstract*—Localization of passive Radio-Frequency Identification (RFID) tags has been used to monitor landslide surface displacement since 5 years. This method, applied on slow displacements lower than 1cm per day, allows a high spatio-temporal resolution at a relatively low cost. With the feedback of the previous years, this paper proposes to summarize the various challenges encountered with the long-term outdoor RFID localization method, and presents data-processing solutions that were implemented to overcome these challenges. We propose a complex-smoothing unwrapping algorithm, a multi-frequency merging operation, as well as multi-tag and multi-antenna phase combining method. The concept of an unwrapping reference guide is presented and applied with groups of tags showing coherent displacements, or with absolute reference measurements. These approaches allow a higher data availability up to 38% for one site over multiple years, and a better phase unwrapping. Earth surface displacement monitoring with RFID proves to be a robust and accurate solution, with four equipped sites across France and Switzerland.**

***Index Terms*—Phase localization, phase unwrapping, data processing, landslides, RFID, remote sensing, early warning**

I. Introduction

Radio-Frequency Identification (RFID) has recently drawn the attention of the Earth Sciences community [1], notably for environment remote sensing at low cost. RFID tag localization has been a growing research topic in the past years [2], with multiple localization methods [3], [4] and applications [5], [6]. Apart from solely localization-based monitoring, RFID technology is foreseen as a promising way to perform low-cost and spatially diverse environmental sensing. Notably in outdoors scenarios, long-term RFID monitoring (months to years) in complex environments that generate high measurement noise, is a current and growing research field. In diverse application domains such as infrastructure monitoring [7], agricultural monitoring [8], [9], social insects behavior monitoring [10], ice formation [11] or snow depth monitoring [12], and of course earth surface processes monitoring [1], robust and synthetic RFID information is needed to ensure optimal data continuity and exploitation. Although not focused on displacement monitoring, these applications would clearly benefit from a data availability increase.

In most scientific works regarding RFID localization, the presented datasets show smooth and correctly-sampled measurements that correspond to laboratory-controled

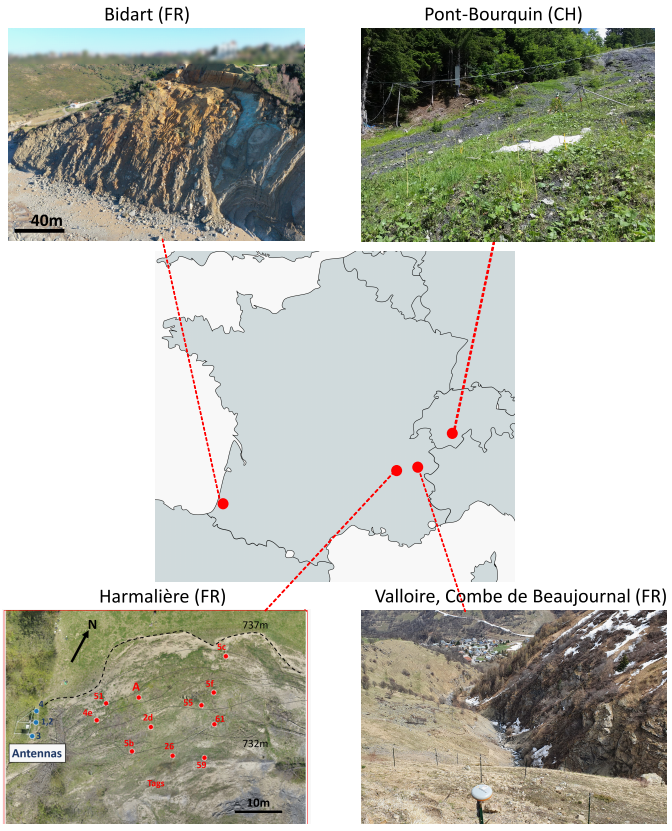

FIG. 1 Map of the RFID-instrumented sites across France and Switzerland, represented as red dots.

experiments [13]–[21]. In real-life scenarios such as retail environments [2] or outdoor landslide monitoring [1], [22], the acquired data is inevitably noisier and intermittent. At the same time, RFID generally yields abundant and redundant data that can enhance the data from each tag [23], [24]. In many cases the objects are monitored by multiple tags, multiple antennas or through multiple carrier frequencies, with the objective of forming tag arrays or yielding more robust data. Moreover as the size of the instrumented sites grow, the overall number of tags also increase, with a growing need for synthesizing redundant data and making

it more exploitable. This data redundancy poses new data processing challenges regarding the reliability of RFID-phase information, especially with regards to phase ambiguity and unwrapping which are crucial elements when recovering tag displacements.

With the combined perspectives of long-term RFID measurements and of data redundancy exploitation, RFID landslide monitoring experiments represent unique candidates for providing long-term, real-life noisy and redundant signals. This method has already proven its centimeter-scale accuracy through multiple works [12], [22], [25], [26]. The feedback offered by the past years of monitoring is of great use for understanding real-application scenarios, especially concerning the process of phase unwrapping.

Several techniques already exist for landslide displacement monitoring, such as optical approaches [27], radar interferometry [28] or GPS [29]. Despite their simplicity, optical methods are sensitive to obstruction by obstacles, fog or heavy rain. Radiofrequency methods are much less sensitive to these obstacles, but they require more complex and expensive systems, and usually rely on active sensors. Compared to these classical methods, RFID monitoring offers a lower-cost alternative in terms of installation and maintenance, because the tags are passive. Additionally, RFID provides dense measurements both in space and time with easy reflector identification, that are little sensitive to obstruction (vegetation, snow cover, fog). This is a great advantage in an all-season long-term monitoring approach.

Among various RFID localization schemes, phase-based methods have shown the best accuracy in outdoor scenarios [25], with centimeter precision. In particular we will use the Time-Domain Phase-Difference (TD-PD) method [2] for its robustness and high precision. The unwrapping process is a central subject in the phase-based RFID localization literature [13], [30]. It is the main step that allows phase data to be interpreted in terms of displacements. The main difficulty that unwrapping poses is that of phase ambiguity, which has been thoroughly investigated in the past years [31], [32]. Recently, several works have focused on exploiting implicit information or bayesian filters in order to improve phase unwrapping even in noisy and multipath-rich environments [33]–[36]. But the challenge of data availability and quality in itself is seldom tackled, being a more *applied* challenge with a strong dependency on the context. It is nonetheless of utmost importance, as in our experience the main causes of unwrapping errors are data gaps and data noise : an absence of data during a rapid tag displacement will very likely generate unwrapping errors, and a very noisy signal will have high chances of being incorrectly unwrapped.

In this paper, which is an extended version of [37], we propose to discuss the recent advances in RFID-phase monitoring as applied to soil surface displacement monitoring using RFID, with data and experience from the past years on several instrumented landslides. We present new algorithms and data processing methods aimed at solving issues concerning RFID data availability and quality. We also propose a discussion on the various ways RFID phase unwrapping can be performed in a diversity of contexts, especially when handling real-life noisy and partial phase data. After presenting the RFID tracking method as applied on different monitored landslides (II), we discuss the different data availability challenges that the method poses as well as the software solutions implemented in order to overcome those challenges (III). The signal processing methods used to obtain robust synthetic measurements are presented, using data fusion and processing algorithms (IV). At every processing step, a short literature review of similar methods is proposed. Most of the presented approaches exploit the high redundancy of RFID data, allowed by the important number of tags that are deployed and by the multiple channels through which the tags are read. The concept of a guide for unwrapping phase data is presented. To our knowledge, this work is the first attempt at applying the concept of an unwrapping guide to RFID data. The data availability improvements obtained for phase data, are quantified and discussed for all instrumented sites (V). These methods, here applied to outdoor long-term monitoring, can be of great use in the implementation of long-term monitoring scenarios in challenging environments.

II. Equipment and localization method

A. RFID Instrumentation

This study will discuss the RFID data from 4 landslides, that all share the same measurement scheme. Several RFID tags (Confidex Survivor) are continuously read by an acquisition system consisting of an interrogator (Impinj SR420 or equivalent) and at least two reader antennas. A micro-computer and a modem ensure continuous data acquisition and transfer.

The measurement rate depends on the site and the available power : autonomous stations relying on solar/wind energy use a lower acquisition frequency than power-grid-connected stations. On average the available data gives a minimum of 100 phase readings per day and per tag. Both the Phase of Arrival (PoA) and the Received Signal Strength (RSSI) are measured, in order to estimate the quality of the received phase signal. All measurements are performed at four different carrier frequencies : 865.7, 866.9, 866.9 and 867.5 MHz in Europe (ETSI EN 302 208).

B. Monitored sites

The four instrumented sites are located across France and Switzerland (see Fig. 1). All sites grossly correspond to the typical setup presented in Figure 2, with a group of tags facing the antennas, placed by pairs on fiber glass or metal stakes at an elevation of approximately 1m above ground. For generalization purposes, these stakes can be simply considered as tagged objects. The reader antennas are positioned on stable ground close to the landslide, usually at a higher altitude than the tags. The tagged objects are placed on (slowly) moving

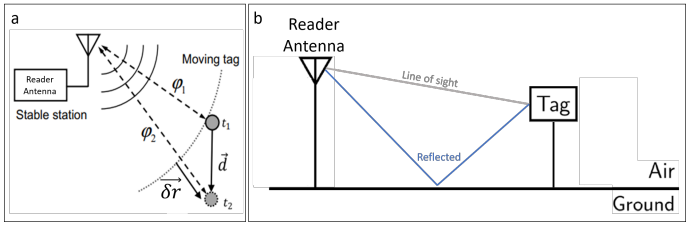

FIG. 2 Schematic principle of all RFID monitoring sites. (a) The principle of relative TD-PD localization : the phase variation between two measurements is linked to the projected radial distance variation (see Equation 1). (b) The tags are placed on the monitored objects (metallic or fiberglass stakes) about 1m above ground, which can generate multipath interference between the line of sight (grey) and reflected (blue) paths.

ground. The maximum read range for the system is about 50-60m.

The main objective of our approach is to monitor each tagged object (metallic stake equipped of two tags) individually through time. In reality, a landslide usually consists of one or multiple blocks. Tagged objects on the same block behave the same way, and hence present coherent displacements.

In all the presented cases, the landslide general movement is known *a priori* and the antennas are positioned optimally with regard to this movement. Except from l'Harmalière (see below), the 1D radial distance measured by each antenna roughly corresponds to the landslide movement.

- The Bidart landslide is located on the south-east coast of France. It has been under observation by the Bureau de recherches géologiques et minières (BRGM) and Geolithe, for more than 3 years. The RFID setup was installed in 2022 and consists of 2 reader antennas and about 30 tags. Reference measurements are frequently acquired using GPS and tacheometry. This coastal landslide has shown strong activity since its recent instrumentation, with displacement rates up to 5 meters per year.
- The Harmalière landslide (Sinard, France) is located near Grenoble in the western Pre-Alps, and is a slow moving landslide currently active and investigated by many research projects [38]. The RFID setup, installed in 2020 [22], consists of 4 reader antennas and 32 tags spread in a 30m by 30m investigated zone. Tacheometry reference measurements are frequently performed. The Harmalière landslide RFID experiment was built in a different way than the other RFID sites, with an open multi-antenna setup oriented towards 2D and 3D monitoring [22]. Although this installation was built
- The Pont-Bourquin landslide is located in the western Pre-Alps near Lausanne in Switzerland. The setup installed in 2017 [26], consists of 2 reader antennas and 20 tags. An extensometer located near the installation is used as a 1D-reference for surface displacement (see IV). This reference is notably unavailable during winter due to snow cover on the extensometer wire. This site shows the longest monitoring time, with several data features to interpret : strong acceleration phases, snow creep, harsh weather conditions.
- The Valloire landslide is located in a steep valley (Beaujournal) above the city of Valloire (France). In the case of exceptional rainfall events this landslide threatens to feed debris flow and endanger the city. The site was instrumented in 2019, and features RFID as well as photogrammetry and seismic monitoring instrumentation. The Valloire landslide has not shown measurable activity since its RFID instrumentation.It has nonetheless been an important source of data to test and improve the methods herein presented.

The sites presented above cover a wide variety of topographies, weather conditions and environmental risk, highlighting the versatility of the presented technique.

Amongst other factors, data gaps are often related to the power supply failure of RFID stations. Most stations need to be electrically autonomous due to their location, and this implies the use of in-situ power sources such as wind turbines or solar panels. For such systems where energy is a scarce resource, a compromise is necessary between measurement sampling frequency (which depletes the batteries) and data continuity over time (which requires available battery power). As of now, the measurement scheme has been adapted depending on the power source of each station : the autonomous station in Harmalière was set to a lower sampling frequency (2 minutes of measurement over 20 minutes : 10% duty cycle) than the Pont-Bourquin station (100% duty cycle), which is connected to the Swiss power grid. On an energy-saving setup such as l'Harmalière, the strategy could be further adapted by increasing the sampling frequency when increasing displacements are detected.

C. RFID Relative localization scheme

A schematic of the TD-PD localization method is presented in Figure 2a. TD-PD is a relative ranging technique based on a phase variation $\delta\phi = \phi_2 - \phi_1$ between two measurements of the same moving point, at different points in time. $\delta\phi$ is related to the radial distance variation $\delta r = r_2 - r_1$ between the tag and the reader antenna, by the following equation:

$$\delta r = -\frac{c}{4\pi f}\delta\phi \tag{1}$$

where f is the frequency of the electromagnetic wave (in Europe 865.7, 866.9, 866.9 or 867.5 MHz) and c is the speed of light in the propagation medium. It is important to note that Eq.(1) is only valid for displacements smaller than $\lambda/4 \approx 8$ cm between two phase measurements because of phase ambiguity. This ambiguity which should ideally be $\lambda/2$, is further reduced due to the reader setup used. In the present case the $\lambda/4$ condition is generally fulfilled as the incremental displacements are small compared to the wavelength (usually less than 1 cm between two successive acquisitions). In the

case where the phase is correctly unwrapped, Eq.(1) is valid for any unwrapped phase variation. Phase unwrapping is a crucial step in recovering true tag displacement, as we will see below (IV).

III. Challenges for RFID data availability

This section will present and discuss the main challenges encountered with the RFID-phase monitoring technique, in terms of data availability, quality and processing.

A. Increase data availability with multiple antennas and tags

The availability of data at all times is crucial in the context of early warning systems, especially at the start of a soil surface movement. The quality of the signal is usually worse during strong precipitation events, when the risk of landslide activation is generally higher [39]. Additionally, the experience showed that RFID phase availability is heavily dependent on tag/antenna orientation and multipath shading. In order to increase data availability and redundancy, most sites were equipped with two tags per monitored object, at a short distance from one another (about 20-50cm). Additionally, multiple antennas often read the same tag, providing more data redundancy. This alone can mitigate several problems : the multipath-induced artifacts can be detected and compensated, and the data availability is higher which can further increase the continuity of the displacement measurement (see section IV).

In all the following sections, data availability does not refer to the sheer amount of acquired data. Rather, it reflects the fact that at any point in time, there is an available data point for every monitored object.

B. Avoid unwrapping errors due to data gaps

Data continuity over long periods of time is a key challenge in order to correctly estimate tag displacement. In the TD-PD relative localization scheme, the maximum readable displacement between two measurements is limited to a few centimeters. When a data gap coincides with a rapid displacement higher than the unwrapping ambiguity, this localization scheme alone does not allow true displacement estimation. Such data gaps can be caused by various phenomena such as hardware failures, multipath shading, or harsh environmental conditions.

The unwrapping ambiguity is geometrically dependent on the angle between tag displacement and antenna-to-tag radial vector. In the Harmalière landslide [22], a multi-antenna setup is described with a localization approach taking advantage of the Angle-of-Arrival concepts [40], although the distance between the antennas is much higher than the required distance for an Angle-Of-Arrival solution. The system aperture is parallel to the tags displacements, which increases the size of the acceptable ambiguity. In such setups, tags can be tracked even when incremental displacements are higher than $8cm$. The downside of such methods is the higher sensitivity of the localization to a phase measurement error. In order to take advantage of both approaches (Angle-of-Arrival and 1D phase unwrapping), new methods could be developed in the future.

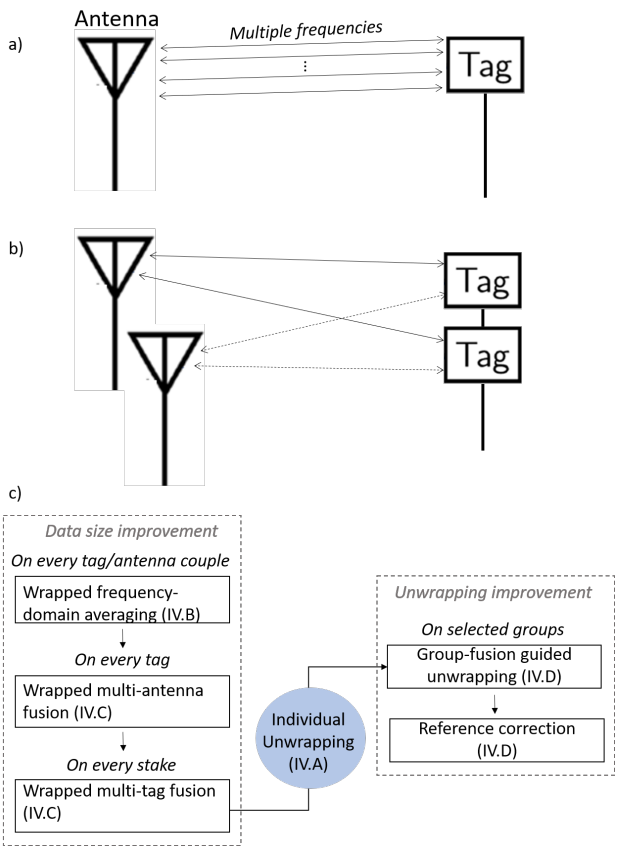

FIG. 3 (a) Schematic of the multi-frequency approach : every tag-antenna couple yields four phase measurement series. (b) Schematic of the multi-tag and multi-antenna approaches. (c) Flowchart for data fusion with all approaches : multi-frequency (MF), multi-antenna (MA), multi-tag (MT) and guided unwrapping.

The next section will describe the various data processing methods that were implemented in order to improve the quality of the RFID data, with an objective of decreasing the number of unwrapping errors and obtaining more synthetic results.

IV. Data fusion and processing

The data continuity and availability issues are mitigated via a signal processing data-fusion approach, notably by taking advantage of the information redundancy provided by a dense network of tags, as well as the multi-frequency and multi-antenna measurements. All these processes will be illustrated by following the data improvement of one specific tagged object (stake) monitored with two tags, in the Pont-Bourquin landslide (see Figures 4 to 6). The overall data workflow is summarized in Figure 3, with simple schematics summarizing the various approaches. At every step of the process, a short and specific literature review will allow to put the proposed method into perspective.

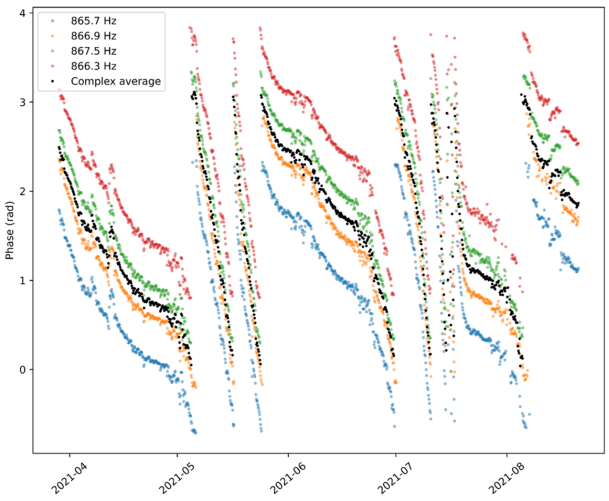

FIG. 4 Phase measurements at four different frequencies and the corresponding fused measurement (black dots) for one tag on the Pont-Bourquin landslide. The initial sampling frequency is one measurement per minute for every tag and antenna couple, but the presented data was resampled for readability. The total displacement is about 60cm. Each frequency channel was offset to increase readability. The best mono-frequency series shows 26111 data points, and the multi-frequency averaging series shows 49055 points.

A. *Complex rolling window unwrapping*

As explained above, phase unwrapping is a very important step in phase processing. Many approaches have been presented in the recent literature to tackle different phase unwrapping situations.

In general, the unwrapping methods based on bayesian state-space models are fit for scenarios where either the antennas or tags move along inertia-dominated paths : flying or sliding object, conveyor belt, unmaned-aerial vehicle equipped with a reader. [31] resolves the phase ambiguity using an Extended Kalman Filter in a multi-antenna, moving-tag scenario with an accuracy of 0.02 m. [33] implements a particle filtering approach with a moving antenna to resolve distance ambiguity, taking into account the potential multipath-rich environments. They reach accuracies around the 0.2 m scale.

Other more deterministic unwrapping methods also exist, often considering the problem as an optimization problem with the objective of linearizing it. Such methods are often sensitive to other reference measurements, such as reference tags or known antenna/tag trajectory. [13] presents an unwrapping algorithm based on the segmentation of the signal in coherent measurement sets. Each segment is first unwrapped with a simple algorithm, then the whole set is unwrapped by minimizing a cost function based on the antenna positions. Predicted accuracy is below 0.1 m.

In order to overcome the errors on reference measurement or due to strong multipath interference, machine learning has also been applied. Notably the tag/antenna displacement trajectories can be taken into account in training the algorithms. For example, [36] performs unwrapping using a random forest algorithm and [41] proposes a deep learning approach, reaching accuracies between 0.5 m and 0.1 m.

In the present scenario, a noise-robust unwrapping algorithm is required, because of the highly variable RFID data quality in an outdoor scenario. We implement an unwrapping algorithm based on a complex smoothing approach. Let ϕ be the measured phase series (from 0 to 2π) and z_ϕ be the corresponding complex angle series :

$$z_\phi = e^{i\phi}$$

We decompose this complex series in a low-frequency smoothed z_s component and a high-frequency $\tilde{z}$ component, in order to avoid discontinuities :

$$z_\phi = z_s + \tilde{z}$$

z_s is obtained by average smoothing over a variable time window, usually ten minutes. After this separation, both components are reverted back to real angle values as ϕ_s and $\tilde{\phi}$.

$$\phi_s = Arg(z_s) \qquad \tilde{\phi} = Arg(\tilde{z})$$

We then unwrap the smoothed component ϕ_s using a classical unwrapping algorithm [42] to obtain the smoothed unwrapped phase ϕ_s^U, to which we add the noise to get the final unwrapped measurement ϕ^U:

$$\phi^U = \phi_s^U + \tilde{\phi}$$

Note that by construction the noisy component $\tilde{\phi}$ is considered smaller than π and does not need unwrapping. This algorithm, although quite simple in its implementation, greatly reduces the influence of data noise on the unwrapping process. Nonetheless it does not reduce the quantity of information, as the high-frequency component is not lost in the process : the smoothing is simply used as a temporary step to increase the unwrapping reliability.

B. *Frequency-domain measurement averaging (MF)*

In this section we describe a method for combining the RFID measurements at different frequencies, in one synthetic phase measurement. This approach is compatible with frequency-hopping [18], and brings the same advantages in terms of mitigating multipath interference [17]. It would benefit even more from a larger frequency band than the ETSI band.

Let us first recall the relationship between phase, radial distance r and carrier frequency [2], related to the Frequency-Difference Phase-Difference (FD-PD) ranging method :

$$r = \frac{c}{4\pi}\frac{d\phi}{df} \tag{2}$$

If we hypothesize that the total distance r presents negligible relative variations over the considered time, we can convert all phase measurements to the same equivalent frequency. More

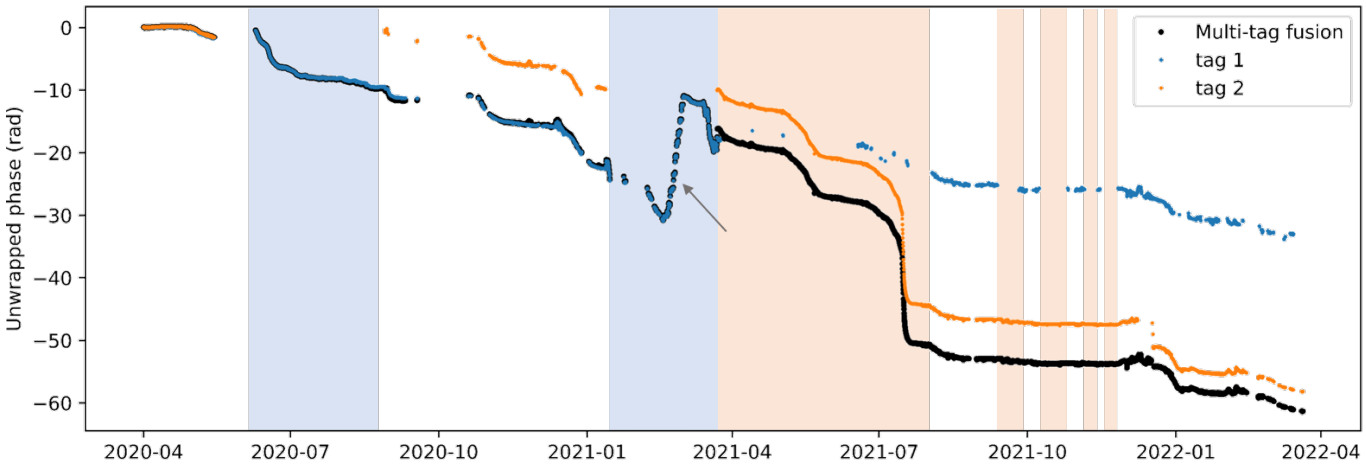

FIG. 5 Unwrapped data series from the two tags on the same object, and the fused measurement (Pont-Bourquin landslide). The background colors highlight the fact that only one tag is read. The steep phase variation (grey arrow) in February 2021 corresponds to snow melt, generating a backwards displacement due to the bending elasticity of the fiber poles holding the tags.

precisely, that is when the displacement measured by the TD-PD method (Eq. 1) is small compared to the absolute distance estimated via the FD-PD method (Eq. 2).

$$\delta r_{_{TD-PD}} << r_{_{FD-PD}}$$

This approximation is accurate in the case of slow moving landslides, where total radial distances are generally higher than 10 m and their monthly variations on the 0.1 m scale. In this situation, the phase difference $\Delta\phi_f$ between a phase series measured at frequency f, and an equivalent frequency f_{eq} (usually set as 865.7 MHz) can be computed :

$$\Delta\phi_f = r(f - f_{eq})\frac{4\pi}{c} \tag{3}$$

Using Eq.(3) all phase series ϕ_f measured at various frequencies f, are superimposed by subtracting the value $\Delta\phi_f$. This subtraction yields $n_{freq} = 4$ superimposed data series (illustrated in Fig.4) that are fused in a frequency-synthetic complex phase series z_{MF} (MF stands for multi-frequency) :

$$z_{MF} = \frac{1}{n_{freq}} \sum_{f=1}^{n_{freq}} e^{i(\phi_f - \Delta\phi_f)}$$

Computing the complex argument of z_{MF} provides a wrapped-phase synthetic measurement. The final wrapped multi-frequency phase fusion ϕ_{MF} result is computed by :

$$\phi_{MF} = Arg(z_{MF})$$

The fusion approach presented above exploits frequency diversity and allows to concatenate all available frequency channels in one measurement, increasing the size of exploitable data by reducing the data gaps, as shown in Figure 4. The method described is valid for other frequency channels, making it usable with any UHF-RFID standard bandwidth. In fact any frequency channel can be used, provided the computed $\Delta\phi_f$ is smaller than π.

In the next section, we propose methods to further merge multi-channel data, using multi-tag and multi-antenna data series.

C. Combining data across space : multiple tags (MT) and reader antennas (MA)

Another common way of enhancing RFID data is to exploit the spatial diversity of reader antennas and tags. Historically, a major step in tag localization was brought by the k-Nearest-Neighbors approach using reference tags [43] and received signal strength measurements. A bayesian filter was added [44] to increase the accuracy from 1 m to about 0.1 m. Using phase measurements, [45] exploits the difference between tags in order to locate them among a grid of already-localized tags. With a flying antenna without onboard accurate positioning they obtain a tag localization accuracy around 0.2 m. [46] exploits the data from different tags in order to perform tag-to-tag relative localization, and obtains a 0.3 m accuracy. Double-tag arrays are also used by [19] in order to solve phase ambiguity and improve localization accuracy up to about 0.2 m.

Antenna spatial diversity is usually exploited in order to perform 2D or 3D localization, with a generally better accuracy when performed in the plane [21], [22]. [17] exploits the data from multiple antennas for phase or distance disambiguation, with a 2D localization accuracy below 10cm. Phase-based relative 2D localization was also performed using multiple antennas for landslide monitoring [22]. [47] uses a trained neural network to perform multi-antenna phase difference hyperbolic positioning, without any given initial position, reaching an accuracy of 0.5 m. [21] performs hyperbolic localization based on multi-antenna measurements, in an indoors Synthetic Aperture Radar approach and with

an accuracy close to the centimeter scale. [15] uses a multi-antenna Synthetic Aperture approach with a Particle Swarm Optimization algorithm [48], reaching a 3D localization accuracy below 0.2 m.

In the present scenario, we exploit both the multi-tag and multi-antenna approaches in order to obtain better unwrapping results. When two antennas (reader or tag) are close together, the measured phase variations are generally similar and can be superimposed after complex mean subtraction. We thus consider that tags on the same object behave similarly, and that all antennas will measure the same phase variation for each specific tag. Note that we do not aim to use the spatial diversity of tags and antennas to localize objects in 2D or 3D space. Rather we intend to maximize 1D data continuity. The 3D case was investigated elsewhere [22].

Figure 5 shows such correspondence for multi-tag fusion, with a difference between the superimposed phases (from tags on the same object) never exceeding 1 rad ; this difference is most likely a combination of multipath interference and small position difference between the two tags. Fusing several partial vectors in complex space, gives rise to an improved synthetic measurement ϕ_{fused}. After the multi-frequency averaging operations are performed, the complex phase series from all tags on the same object are fused by complex superposition and averaging. The fused phase is then unwrapped in order to recover the estimated displacement. If we define the unwrapping algorithm by U (as described in IV-A), the unwrapped phase ϕ^{unw}_{fused} is obtained using the wrapped fused phase ϕ_{fused} :

$$\phi^{unw}_{fused} = U(\phi_{fused})$$

This whole process tends to synthesize all available data from each tagged object, into one displacement indicator. The next section will present various approaches to obtain further information by exploiting the near environment.

D. Guided unwrapping

When individual data series are not dense enough to correctly unwrap the phase (such as in Figure 5), the unwrapping process can be guided using a reference. This reference can be an absolute measurement or a synthetic fusion vector.

The concept a guide for phase unwrapping already exists in 2D interferometry, where unwrapping is equally a crucial step prior to data analysis. For example, [49]–[51] use a quality-guide to unwrap 2D interferograms. This method comes down to using high-quality unwrapped references to progressively unwrap the surroundings. The following methods apply roughly the same concept to the RFID phase data.

This guiding approach is obviously based on the common motion of multiple tagged objects, which is generally observed as the coherent landslide blocks are large. We use this coherence between different displacements, to better unwrap each and every phase data series. Hence the use of grouped-fusion, which is a loose generalization of the multi-tag approach.

a) Grouped fusion for individual unwrapping: In the case of a data gap during a rapid displacement, simply taking data from each object is usually not enough to correctly unwrap the phase. In such situations, one possibility is to implement a fusion operation over a group of tagged objects sharing the same behavior. All measured phases from the group are merged to produce a synthetic guide containing more information than individual phase series. This guide can then help unwrap every individual tag. Let ϕ_t be the phase series from tag t, then the reference group fusion ϕ_{ref} is computed from the rate of change $\dot{\phi}_t$ using a simple average operation :

$$\dot{\phi}_{ref} = \frac{1}{n_t} \sum_{t=0}^{n_t} \dot{\phi}_t \tag{4}$$

With n_t the number of tags in a group, and $\dot{\phi}_{ref}$ the group fusion time derivative. Equation 4 essentially computes an average velocity of the group of tags. ϕ_{ref} is then obtained by time integration, and presents more features than every individual phase series (see Figure 6). This reference is then used as a guide to unwrap the individual series. Using the unwrapping algorithm U as discussed above, guided unwrapping corresponds to the following operation :

$$\phi_g = U(\phi_m - \phi_{ref}) + \phi_{ref} \tag{5}$$

Where ϕ_m is the measured phase and ϕ_g the unwrapped phase guided by ϕ_{ref}. The main idea behind this operation is that if the measured phase presents an unwrapping error, it will be highlighted and corrected by subtraction of the reference which supposedly shows a better phase continuity. Although the unwrapping is not guided by a high-quality reference but rather by a synthetic group reference, this methods yields coherent results even when the reference and the phase series do not fit perfectly (see Figure 6).

b) Absolute reference measurement: When at least one absolute reference measurement (tacheometry, GPS or extensometer) is available on a field, it is used to help unwrap the whole dataset. This was the case in the Pont-Bourquin landslide where absolute displacement data was available (although scarce in time) via an extensometer. If the reference data is continuous in time, guided unwrapping can be performed. If not, discrete corrections are performed either automatically or by manually correcting the phase. This approach allows keeping track of long-term displacements, as shown in Figure 6.

E. Putting things together

All the previously mentioned approaches are integrated in a hierarchical data processing workflow described in Figure 3. The four frequency channels are first fused together to obtain a synthetic phase series for each tag-antenna couple. Next, the data from all antennas are fused for every tag, in order to have one synthetic measurement for each tag. Then the tags from each object are fused together, and the resulting series are unwrapped by complex unwrapping. Finally, on sites where it is applicable, guided unwrapping is performed using an absolute reference, a group-fusion guide or both.

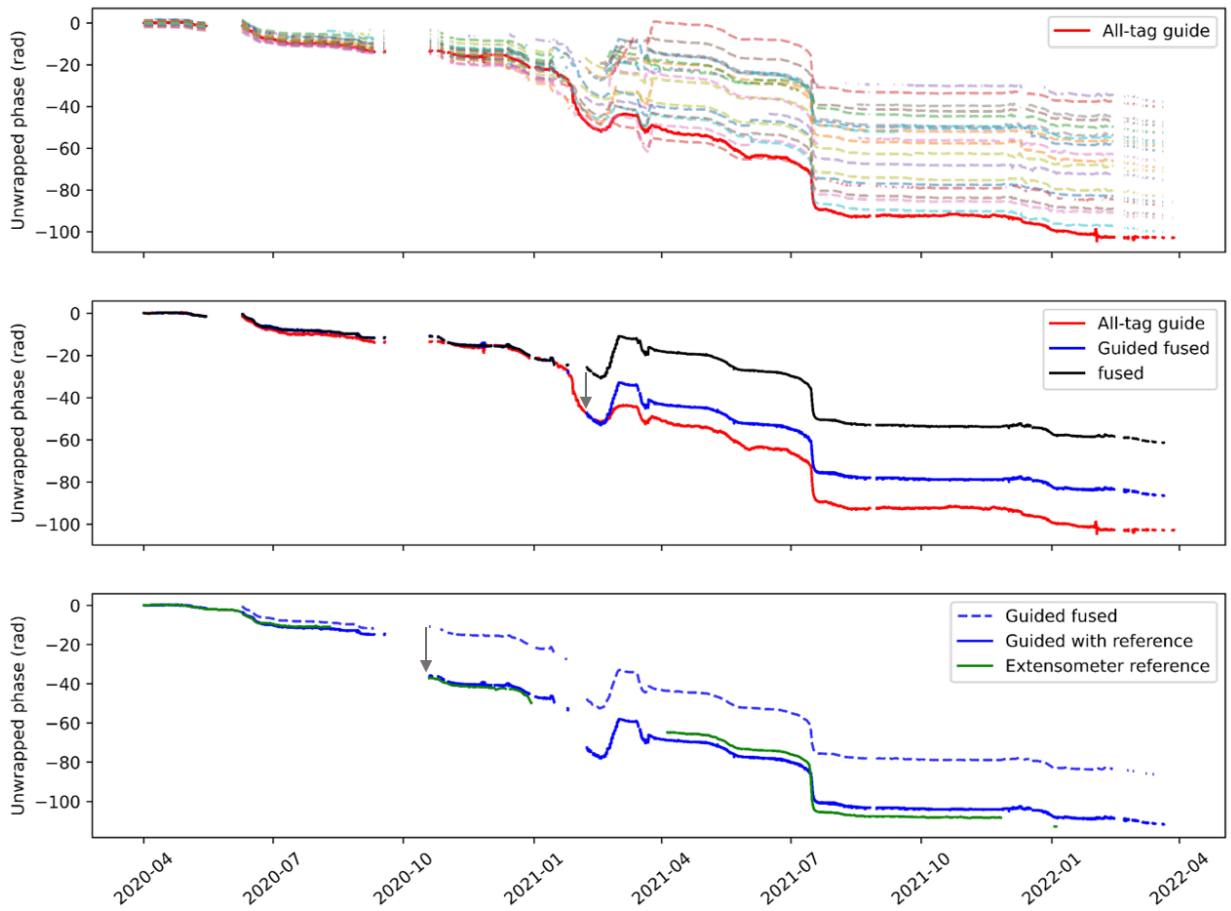

FIG. 6 Example of guided unwrapping process for one tag on the Pont-Bourquin landslide. (Top) Computation of a group-guide based on all phase data. The group is shown in red, and each dotted color line represents a tagged object. (Middle) Guided unwrapping of the single multi-tag data ("fused" in black, see Figure 5) using the group guide in red. The result is in blue. (Bottom) Guided unwrapping using the extensometer data (in green) ; the dotted blue line corresponds to the full blue line in the middle plot ; the final result is again in full blue. The main unwrapping corrections are highlighted by a grey arrow.

V. RESULTS AND DISCUSSION

In this section we present and discuss the results obtained after the phase processing. First we describe the specific data quality and unwrapping improvements concerning one specific tag, then we present and discuss the general improvements brought on all instrumented landslides. Finally we come back to the other monitoring challenges on landslides, and the implemented solutions.

A. Data availability improvement and unwrapping for one tag

Figure 4 presents each frequency channel for one tag, and the corresponding MF phase series during a 5-month period. Over this small time period, the MF fusion yields an available and continuous data size 80% larger than the mono-frequency phase series : the best individual series shows 26111 data points, and the MF fusion shows 49055.

The unwrapped multi-tag (MT) fusion results are shown in Figure 5 for the same tagged object, with several corrected unwrapping errors compared to the two individual data series. The noisy variations occurring around March 2021 correspond to snow melt before the metallic stakes were installed, and an unwrapping error (June 2020) remains in the final data. We note that the partially-observed displacement originating from snow creep (February-March 2021), generates unwrapping errors : the total displacement after winter is lower than before winter. This issue is partially solved by using the group-guide on all tags from the Pont-Bourquin landslide : on Figure 6, we see that the whole winter period is covered by the guide, and yields a more coherent displacement after snow creep. Furthermore, the extensometer reference measurements allow for long-term phase correction, notably after September 2020 where displacements occurred but where not measured.

B. General improvement on all sites

Table I shows the general data availability improvement of the fusion approach on all 4 sites. Each layer increases the exploitable data by the given percentage. We can note

Processing step	Pont-Bourquin	Valloire	Harmalière	Bidart
MF (%)	13 (26)	23 (48)	2 (10)	2 (13)
MA (%)	4 (19)	2 (30)	3 (18)	3 (31)
MT (%)	15 (58)	2 (22)	2 (18)	-
ALL (%)	38 (129)	28 (64)	3 (50)	5 (37)

TABLE I Overall available data size improvement for each processing layer compared to the previous one, for the four RFID-instrumented sites. The increase is given in percentage of average data availability increase, with the maximum value in parenthesis. Pont-Bourquin landslide : 5-year monitoring period and 20 tags. Valloire landslide : 1-year period and 15 tags (MT and MA are cumulated because of their low value). Harmalière : 2-year period and 15 tags. Bidart : 10-month period and 40 tags (no multi-tag available).

that for Valloire and Pont-Bourquin, the multi-frequency (MF) fusion brings a high data availability increase above 10%. Comparatively the multi-antenna (MA) fusion does not bring a significant improvement on average, with some individual exceptions especially on Valloire (+30%) and in Bidart (+31%).
In total the three processing layers (ALL) increase the data availability by 3 to 38% depending on the site, with peaks for specific objects reaching more than 50% data availability increase.

As seen in Figure 6, the use of a synthetic guide allows a better signal reconstruction by reducing the number of unwrapping errors. In the Bidart landslide, the data was split in two distinct groups of tags with coherent behaviour, in order to unwrap the data using a group-guide. The improvements obtained by this method are quantified in Table II, compared to the previous processing which consisted of individual mono-frequency series unwrapping. This shows a strong reduction of detected cumulative unwrapping errors. These errors are computed based on reference measurements over a 2 months period with displacements of about 1m, from March to May 2022.

Figure 7 compares the data availability improvement to the normalized read rate for each and every tag. The normalized read rate is computed by comparing the number of measurements to the ideal number (with no data gap) expected on the measurement period. As could be expected, we note that the processing is least beneficial to the tagged objects with the best read rates ; on the contrary, the data availability increase is much higher for tags with low read rates.

C. Discussion

Figure 7 shows that the main benefits of the fusion approach arise in the scenario of a difficult tag reading, e.g. when multipath interference is strong or when the signal strength is poor. In most cases this occurs on tag that are either at a great distance from the antenna, or when the read angle is high. The increase in data robustness is clearly highlighted in such situations. We also note that several tags with the lowest read rates (close to 0.1) do not benefit as much from the processing.

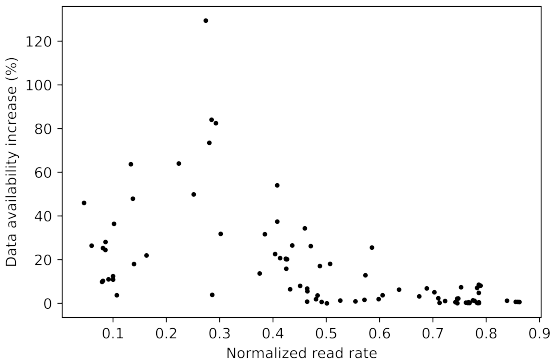

FIG. 7 Data availability increase in percentage after applying the MF/MA/MT processing, as a function of the normalized read rate for every site.

We now turn to a more specific discussion on the processing steps, based on the results from Table I.

The MF fusion is the main contribution to data availability increase. Table III shows the cumulative improvement brought by each new frequency channel, on the Pont-Bourquin site. This highlights that frequency diversity is a major aspect, and that even broader frequency windows would further improve the data availability. The MF fusion approach yields much better results on Pont-Bourquin and Valloire than on the two other sites. This is most likely due to the environmental conditions on these two sites : a higher altitude with stronger presence of snow. The corresponding multipath effects and signal strength diminution, although not critical in general, can worsen the data quality in already deteriorated situations. In such scenarios, the multi-frequency approach proves to be valuable.

The relatively low increase from the MA processing on all sites, is most likely due to the nature of the general measurement setup : antennas are the same model and often rather close together. Hence the situations where one antenna reads a tag and not the others are rare.

We note that the multi-tag (MT) fusion brings a highly variable improvement. This can be explained by the height difference between tags on an object : the objects shaded by multipath interference or micro-topography will greatly benefit from MT fusion, whereas those that are in a better radio-frequency environment will not. Also, in cases where the lowest of the two tags is poorly read, the MT fusion will not bring significant improvements either, because most of the data comes from the topmost tag.

Moreover, Table I shows that the data from l'Harmalière and Bidart benefit much less from the processing, than the two other sites. This is most likely because both setups were already optimized to obtain the highest reading availability : relatively short distances between antenna and tags, more overall measurements thanks to higher number of antennas, as well as tag and antenna orientation optimization.

Measurement quality and trueness is also sensitive to multipath interference, which is a general challenge in RFID localization [14]. Multipath is related to terrain topography, system geometry, but also to soil humidity and snow cover. As studied in [22] multipath generates both a measurement bias, a higher random error and a potential data loss due to the weak signal. The measurement errors amount to a centimeter-scale localization error in the horizontal plane. As of now, the presented data processing scheme can mitigate some of these effects : the multi-frequency approach takes advantage of the different multipath behavior with varying frequency, and the multi-tag and multi-antenna approaches yield a more multipath-robust measurement thanks to spatial diversity.

Environmental conditions can also have a strong influence on RFID-phase measurements. Phase random fluctuations can imply centimeter value errors in localization, as studied in [25]. This study confirms the need for using appropriate hardware for outdoor phase-stable RFID measurements. The main limitation to a spatial up-scaling of the method is the tag reading range. The current method cannot read the Survivor RFID tags past a 60m maximum distance, which limits the size of the monitored field. The reader antennas directivity can also limit the angular range, both horizontally and vertically.
In order to increase the size of the monitored areas, long-range tags were installed along with a more sensitive reader (Impinj R700). For even wider areas, new methods are developped based on Unmaned Aerial Vehicle (UAV), as described in [1], [52].

Figure 8 illustrates a portion of the final results for the Pont-Bourquin landslide. Through this figure we do not claim to present quantitative results concerning the localization accuracy of the RFID monitoring approach. Ideally speaking, the validation of our approach would necessitate independent reference measurement on the position of each tag, which is hardly feasible for technical and economical reasons. Nevertheless we point out that this method has already proven its centimeter-scale accuracy through multiple works [22], [25], [26], and that the present paper mostly aims at enhancing phase data.

Unwrapping errors	Before	After
Bidart Group 1	11	3
Bidart Group 2	7	3

TABLE II Number of cumulative detected unwrapping errors with and without applying the grouped fusion, for two different groups of tags in the Bidart landslide.

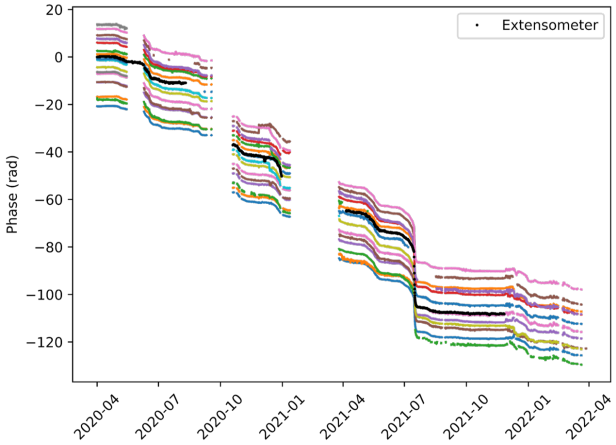

FIG. 8 Final results from the last two years of RFID data on the Pont-Bourquin site. Each colored line represents the displacement of a tagged object, after all processing (MF, MA then MT) and after guided unwrapping with the group-guide and extensometer data (black line). An offset was added to every data series to increase readability.

Nb of frequencies used	2	3	4
Data availability increase (%)	8	11	13

TABLE III Cumulative data availability increase brought by the MF processing on Pont-Bourquin, depending on the number of frequency channels taken into account.

VI. Conclusion and perspectives

This paper proposes various data processing and fusion techniques, that take advantage of the RFID data redundancy in order to increase data availability and quality. These approaches are based on multi-source (frequency/antenna/tag) data fusion and on phase calibration using various references, with an objective of both increasing the available data size and decreasing the number of phase unwrapping errors. By applying such methods to RFID phase-based landslide monitoring, we show that these processes are valuable in long-term outdoor and complex environments. The overall average data availability improvement of the process was between 3% and 38% depending on the site, with several monitored objects greatly benefiting from the processes (+50% data availability). Moreover, the process yields more synthetic data which is therefore more exploitable.

Earth surface displacement monitoring with RFID has proven to be a viable solution, with four equipped sites across France and Switzerland. The varying nature of outdoor RFID data quality, will bring us to further develop data fusion approaches. In particular we foresee that applying bayesian filters to such measurement systems is a promising path.

VII. Acknowledgements

We would like to express special thanks to the BRGM, the INTERREG SUDOE (2019-2022) project RISK COAST and Geolithe, for allowing us to present their data. We would also like to thank the Geophysical Instrumentations group at ISTerre for their contribution to the Harmalière and Pont-Bourquin stations. This work was partially funded by the ANR LABCOM GEO3ILAB, Geolithe and by the Region Auvergne Rhone-Alpes RISQID project.

References

[1] M. L. Breton, F. Liébault, L. Baillet, A. Charléty, Éric Larose, and S. Tedjini, "Dense and longdterm monitoring of earth surface processes with passive rfid – a review," 2021.

[2] P. V. Nikitin, R. Martinez, S. Ramamurthy, H. Leland, G. Spiess, and K. Rao, "Phase based spatial identification of uhf rfid tags," in *2010 IEEE International Conference on RFID (IEEE RFID 2010)*, pp. 102–109, IEEE, 2010.

[3] M. Scherhäufl, M. Pichler, and A. Stelzer, "Uhf rfid localization based on evaluation of backscattered tag signals," *IEEE Transactions on Instrumentation and Measurement*, vol. 64, no. 11, pp. 2889–2899, 2015.

[4] N. D. Rohmat Rose, T. J. Low, and M. Ahmad, "3d trilateration localization using rssi in indoor environment," *International Journal of Advanced Computer Science and Applications*, vol. 11, no. 2, pp. 385–391, 2020.

[5] L. Vojtech, M. Nerada, J. Hrad, and R. Bortel, "Outdoor localization technique using active rfid technology aimed for security and disaster management applications," in *Proceedings of the 2015 16th International Carpathian Control Conference (ICCC)*, pp. 586–589, IEEE, 2015.

[6] A. Buffi, P. Nepa, and F. Lombardini, "A phase-based technique for localization of uhf-rfid tags moving on a conveyor belt: Performance analysis and test-case measurements," *IEEE Sensors Journal*, vol. 15, no. 1, pp. 387–396, 2014.

[7] C. Strangfeld, S. Johann, and M. Bartholmai, "Smart rfid sensors embedded in building structures for early damage detection and long-term monitoring," *Sensors*, vol. 19, no. 24, p. 5514, 2019.

[8] F. Deng, P. Zuo, K. Wen, and X. Wu, "Novel soil environment monitoring system based on rfid sensor and lora," *Computers and Electronics in Agriculture*, vol. 169, p. 105169, 2020.

[9] R. Rayhana, G. Xiao, and Z. Liu, "Rfid sensing technologies for smart agriculture," *IEEE Instrumentation & Measurement Magazine*, vol. 24, no. 3, pp. 50–60, 2021.

[10] P. Nunes-Silva, M. Hrncir, J. Guimarães, H. Arruda, L. Costa, G. Pessin, J. Siqueira, P. De Souza, and V. Imperatriz-Fonseca, "Applications of rfid technology on the study of bees," *Insectes sociaux*, vol. 66, no. 1, pp. 15–24, 2019.

[11] M. Wagih and J. Shi, "Wireless ice detection and monitoring using flexible uhf rfid tags," *IEEE Sensors Journal*, vol. 21, no. 17, pp. 18715–18724, 2021.

[12] M. Le Breton, É. Larose, L. Baillet, Y. Lejeune, and A. van Herwijnen, "Monitoring snowpack swe and temperature using rfid tags as wireless sensors," *EGUsphere*, pp. 1–24, 2022.

[13] A. Tzitzis, S. Megalou, S. Siachalou, T. G. Emmanouil, A. Kehagias, T. V. Yioultsis, and A. G. Dimitriou, "Localization of rfid tags by a moving robot, via phase unwrapping and non-linear optimization," *IEEE Journal of Radio Frequency Identification*, vol. 3, no. 4, pp. 216–226, 2019.

[14] E. DiGiampaolo and F. Martinelli, "A multiple baseline approach to face multipath," *IEEE Journal of Radio Frequency Identification*, vol. 4, no. 4, pp. 314–321, 2020.

[15] A. Tzitzis, A. R. Chatzistefanou, T. V. Yioultsis, and A. G. Dimitriou, "A real-time multi-antenna sar-based method for 3d localization of rfid tags by a moving robot," *IEEE Journal of Radio Frequency Identification*, vol. 5, no. 2, pp. 207–221, 2021.

[16] A. R. Chatzistefanou, A. Tzitzis, S. Megalou, G. Sergiadis, and A. G. Dimitriou, "Trajectory-tracking of uhf rfid tags, exploiting phase measurements collected from fixed antennas," *IEEE Journal of Radio Frequency Identification*, vol. 5, no. 2, pp. 191–206, 2021.

[17] S. Yang, M. Jin, Y. He, and Y. Liu, "Rf-prism: Versatile rfid-based sensing through phase disentangling," in *2021 IEEE 41st International Conference on Distributed Computing Systems (ICDCS)*, pp. 1053–1063, IEEE, 2021.

[18] X. Li, Y. Zhang, and M. G. Amin, "Multifrequency-based range estimation of rfid tags," in *2009 IEEE International Conference on RFID*, pp. 147–154, IEEE, 2009.

[19] Y. Zeng, X. Chen, R. Li, and H.-Z. Tan, "Uhf rfid indoor positioning system with phase interference model based on double tag array," *IEEE Access*, vol. 7, pp. 76768–76778, 2019.

[20] C. Peng, H. Jiang, and L. Qu, "Deep convolutional neural network for passive rfid tag localization via joint rssi and pdoa fingerprint features," *IEEE Access*, vol. 9, pp. 15441–15451, 2021.

[21] P. Tripicchio, S. D'Avella, and M. Unetti, "Efficient localization in warehouse logistics: a comparison of lms approaches for 3d multilateration of passive uhf rfid tags," *The International Journal of Advanced Manufacturing Technology*, vol. 120, no. 7, pp. 4977–4988, 2022.

[22] A. Charléty, M. Le Breton, E. Larose, and L. Baillet, "2d phase-based rfid localization for on-site landslide monitoring," *Remote Sensing*, vol. 14, no. 15, p. 3577, 2022.

[23] L. Qiu, X. Liang, and Z. Huang, "Patl: A rfid tag localization based on phased array antenna," *Scientific Reports*, vol. 7, no. 1, pp. 1–12, 2017.

[24] Y. Zhang, L. Xie, Y. Bu, Y. Wang, J. Wu, and S. Lu, "3-dimensional localization via rfid tag array," in *2017 IEEE 14th international conference on mobile ad hoc and sensor systems (MASS)*, pp. 353–361, IEEE, 2017.

[25] M. Le Breton, L. Baillet, E. Larose, E. Rey, P. Benech, D. Jongmans, and F. Guyoton, "Outdoor uhf rfid: Phase stabilization for real-world applications," *IEEE Journal of Radio Frequency Identification*, vol. 1, no. 4, pp. 279–290, 2017.

[26] M. Le Breton, L. Baillet, E. Larose, E. Rey, P. Benech, D. Jongmans, F. Guyoton, and M. Jaboyedoff, "Passive radio-frequency identification ranging, a dense and weather-robust technique for landslide displacement monitoring," *Engineering geology*, vol. 250, pp. 1–10, 2019.

[27] M. Jaboyedoff, T. Oppikofer, A. Abellán, M.-H. Derron, A. Loye, R. Metzger, and A. Pedrazzini, "Use of lidar in landslide investigations: a review," *Natural hazards*, vol. 61, no. 1, pp. 5–28, 2012.

[28] O. Monserrat, M. Crosetto, and G. Luzi, "A review of ground-based sar interferometry for deformation measurement," *ISPRS Journal of Photogrammetry and Remote Sensing*, vol. 93, pp. 40–48, 2014.

[29] J. A. Gili, J. Corominas, and J. Rius, "Using global positioning system techniques in landslide monitoring," *Engineering geology*, vol. 55, no. 3, pp. 167–192, 2000.

[30] H. Wu, B. Tao, Z. Gong, Z. Yin, and H. Ding, "A fast uhf rfid localization method using unwrapped phase-position model," *IEEE Transactions on Automation Science and Engineering*, vol. 16, no. 4, pp. 1698–1707, 2019.

[31] S. Sarkka, V. V. Viikari, M. Huusko, and K. Jaakkola, "Phase-based uhf rfid tracking with nonlinear kalman filtering and smoothing," *IEEE Sensors Journal*, vol. 12, no. 5, pp. 904–910, 2011.

[32] M. Scherhäufl, M. Pichler, and A. Stelzer, "Uhf rfid localization based on phase evaluation of passive tag arrays," *IEEE Transactions on Instrumentation and Measurement*, vol. 64, no. 4, pp. 913–922, 2014.

[33] E. Giannelos, E. Andrianakis, K. Skyvalakis, A. G. Dimitriou, and A. Bletsas, "Robust rfid localization in multipath with phase-based particle filtering and a mobile robot," *IEEE Journal of Radio Frequency Identification*, vol. 5, no. 3, pp. 302–310, 2021.

[34] A. J. Hoffman and N.-P. Bester, "Rss and phase kalman filter fusion for improved velocity estimation in the presence of real-world factors," *IEEE Journal of Radio Frequency Identification*, vol. 5, no. 1, pp. 75–93, 2020.

[35] B. Tao, H. Wu, Z. Gong, Z. Yin, and H. Ding, "An rfid-based mobile robot localization method combining phase difference and readability," *IEEE Transactions on Automation Science and Engineering*, vol. 18, no. 3, pp. 1406–1416, 2020.

[36] C. Li, E. Tanghe, P. Suanet, D. Plets, J. Hoebeke, E. De Poorter, and W. Joseph, "Reloc 2.0: Uhf-rfid relative localization for drone-based inventory management," *IEEE Transactions on Instrumentation and Measurement*, vol. 70, pp. 1–13, 2021.

[37] A. Charléty, M. Le Breton, L. Baillet, and E. Larose, "Long-term monitoring of soil surface deformation with rfid," in *2022 IEEE 12th International Conference on RFID Technology and Applications (RFID-TA)*, pp. 101–104, IEEE, 2022.

[38] S. Fiolleau, D. Jongmans, G. Bièvre, G. Chambon, P. Lacroix, A. Helmstetter, M. Wathelet, and M. Demierre, "Multi-method investigation of mass transfer mechanisms in a retrogressive clayey landslide (harmalière, french alps)," *Landslides*, vol. 18, no. 6, pp. 1981–2000, 2021.

[39] F. Guzzetti, S. Peruccacci, M. Rossi, and C. P. Stark, "Rainfall thresholds for the initiation of landslides in central and southern europe," *Meteorology and atmospheric physics*, vol. 98, no. 3, pp. 239–267, 2007.

[40] S. Azzouzi, M. Cremer, U. Dettmar, R. Kronberger, and T. Knie, "New measurement results for the localization of uhf rfid transponders using an angle of arrival (aoa) approach," in *2011 IEEE International Conference on RFID*, pp. 91–97, IEEE, 2011.

[41] C. Li, E. Tanghe, P. Suanet, D. Plets, J. Hoebeke, L. Martens, E. De Poorter, and W. Joseph, "Deep learning enables robust drone-based uhf-rfid localization in warehouses," in *2022 3rd URSI Atlantic and Asia Pacific Radio Science Meeting (AT-AP-RASC)*, pp. 1–4, IEEE, 2022.

[42] "Python. numpy unwrap." https://numpy.org/doc/stable/reference /generated/numpy.unwrap.html Accessed: 2022-11-16.

[43] L. M. Ni, Y. Liu, Y. C. Lau, and A. P. Patil, "Landmarc: Indoor location sensing using active rfid," in *Proceedings of the First IEEE International Conference on Pervasive Computing and Communications, 2003.(PerCom 2003).*, pp. 407–415, IEEE, 2003.

[44] H. Xu, Y. Ding, P. Li, R. Wang, and Y. Li, "An rfid indoor positioning algorithm based on bayesian probability and k-nearest neighbor," *Sensors*, vol. 17, no. 8, p. 1806, 2017.

[45] S. Siachalou, S. Megalou, A. Tzitzis, E. Tsardoulias, A. Bletsas, J. Sahalos, T. Yioultsis, and A. G. Dimitriou, "Robotic inventorying and localization of rfid tags, exploiting phase-fingerprinting," in *2019 IEEE International Conference on RFID Technology and Applications (RFID-TA)*, pp. 362–367, IEEE, 2019.

[46] C. Li, E. Tanghe, D. Plets, P. Suanet, J. Hoebeke, E. De Poorter, and W. Joseph, "Repos: Relative position estimation of uhf-rfid tags for item-level localization," in *2019 IEEE International Conference on RFID Technology and Applications (RFID-TA)*, pp. 357–361, IEEE, 2019.

[47] S. Megalou, A. R. Chatzistefanou, A. Tzitzis, A. Malama, T. Yioultsis, and A. G. Dimitriou, "Hyperbolic positioning and tracking of moving uhf-rfid tags by exploiting neural networks," in *2022 16th European Conference on Antennas and Propagation (EuCAP)*, pp. 01–05, IEEE, 2022.

[48] F. Bernardini, A. Buffi, A. Motroni, P. Nepa, B. Tellini, P. Tripicchio, and M. Unetti, "Particle swarm optimization in sar-based method enabling real-time 3d positioning of uhf-rfid tags," *IEEE Journal of Radio Frequency Identification*, vol. 4, no. 4, pp. 300–313, 2020.

[49] H. Wang, J. B. Weaver, I. I. Perreard, M. M. Doyley, and K. D. Paulsen, "A three-dimensional quality-guided phase unwrapping method for mr elastography," *Physics in Medicine & Biology*, vol. 56, no. 13, p. 3935, 2011.

[50] T. Liu, Z. Shang, J. Wu, D. Zhou, and S. Yan, "Improved branch-cut phase unwrapping strategy based on dynamic adjacent table," *The Journal of Engineering*, vol. 2019, no. 19, pp. 5805–5809, 2019.

[51] P. Ajourlou, S. Samiei Esfahany, and A. Safari, "A new strategy for phase unwrapping in insar time series over areas with high deformation rate: Case study on the southern tehran subsidence.," *International Archives of the Photogrammetry, Remote Sensing & Spatial Information Sciences*, 2019.

[52] A. Buffi, A. Motroni, P. Nepa, B. Tellini, and R. Cioni, "A sar-based measurement method for passive-tag positioning with a flying uhf-rfid reader," *IEEE Transactions on Instrumentation and Measurement*, vol. 68, no. 3, pp. 845–853, 2018.